

Multi-objective Optimization of a Magneto-rheological Prosthetic Knee Actuator

Ketill H. Gudmundsson^{1*}, Fjola Jonsdottir¹, and Sigurdur Olafsson²

¹ Department of Mechanical Engineering, Hjardarhaga 6, 107 Reykjavik, University of Iceland, Iceland.
Tel. (354) 564 1224, Fax. (354) 525 4632, E-mail: ketillh@gmail.com.

² Ossur Inc., Iceland.

ABSTRACT

Regaining biomechanical function, comfort and quality of life is a prime consideration when designing prosthetic limbs. Recently, microprocessor-controlled prosthetic knees, which rely on magneto-rheological (MR) technology, have become available and have the potential to meet these needs. One of these promising products is a prosthetic knee manufactured by the company Ossur Inc. The knee is a synergy of artificial intelligence, advanced sensors and MR actuator technology. The prosthetic knee uses the variable rheological properties of MR fluids to control the knee's variable stiffness while an amputee walks. The fluid has response time in the order of milliseconds, making it possible to vary the knee's stiffness in real-time, depending on sensors data. The focus of this paper is on the MR actuator in the prosthetic knee. The actuator is a variable stiffness MR rotary brake, utilizing MR fluids in shear-mode. MR fluids are fluids that change their rheological properties upon the application of a magnetic field. MR fluids consist of a carrier liquid, immersed with solid particles. The paper addresses the design of the MR rotary brake actuator, with respect to three important qualities. The three design qualities are the maximum obtainable field-induced braking torque of the actuator, the minimum obtainable stiffness in the absence of a magnetic field, and the weight of the MR actuator. It is important to investigate the trade-offs between these qualities. Maximizing the field-induced braking torque of the knee is important for the knee to be capable of supporting heavy amputees. Minimizing the off-state stiffness of the knee is important for fast movements of the knee, in load-free movements. Furthermore, minimizing the weight of the actuator is important for patients comfort. It is realized that these design goals can not be addressed separately and to some extent, the design goals are contradictory. Mathematical models are presented that describe the design goals as a function of selected design parameters. Determining the field-induced braking torque requires a magnetic finite element analysis to evaluate the magnetic flux density in the MR fluid and the shear-yield stress curve of the MR fluid. Evaluating the off-state stiffness requires the off-state viscosity of the MR fluid, along with friction in bearings and oil seals. Calculating the weight of the actuator requires the geometry of the actuator and the density of its materials. The actuator employs a silicone-based MR fluid. The presented models rely on off-state viscosity measurements of an MR fluid from the actuator. The field-induced behavior of the fluid is determined with a shear-yield stress model of a perfluorinated polyether-based (PFPE) MR fluid. The maximum torque, the minimum torque and the weight of the actuator are specified mathematically in the form of three objective functions. A direct search optimization algorithm is presented that investigates, simultaneously, the trade-offs between the three objective functions. The optimization is restricted by practical manufacturing design constraints. Mapping the dependency between the maximum torque, minimum stiffness and the weight of the MR actuator gives valuable insight into further development of the prosthetic knee.

Keywords: MR fluids, actuators, prosthetics, modeling, optimization.

1. INTRODUCTION

Magneto-rheological (MR) fluids are a class of smart materials that are widely being used to make structures adaptive and controllable by a magnetic field. The rheological properties of the MR fluid can be controlled with a magnetic field. An MR fluid consists of a carrier liquid immersed with ferromagnetic micron sized particles. With the application of a magnetic field, the particles are drawn together in electromagnetic chains. Hence, the stronger the magnetic flux in the fluid, the stronger the particle chains. The carrier liquid can be a fluid of various types. The literature describes, for example, silicone-based [1], hydrocarbon-based [1], water-based [1], perfluorinated polyether (PFPE)-based [2] and glycol-based [3] carrier liquids. It has been reported that the carrier liquid does not greatly affect the field-induced strength of MR fluids [4], but on the contrary, greatly affects the off-state viscosity [2]. The carrier liquid used in this study is PFPE-based and the particles are carbonyl iron particles with a size of 1-3 microns. The amount of carbonyl iron particle, in the MR fluid of the current study, is approximately 50% by weight. The properties of the MR fluid are not varied. The optimization varies the geometry of MR prosthetic knee actuator, shown in Figure 1, and assumes a constant MR fluid [5] with constant properties. This involves an optimization of the magnetic circuit, the configuration of the fluid chamber and the weight of the actuator. The magnetic circuit design of an MR rotary brake actuator, used in the prosthetic knee, has been investigated with respect to strength of the actuator [6,7]. The current study takes a wider perspective, looking at the off-state minimum stiffness and the weight of the actuator, along with the field-induced strength.

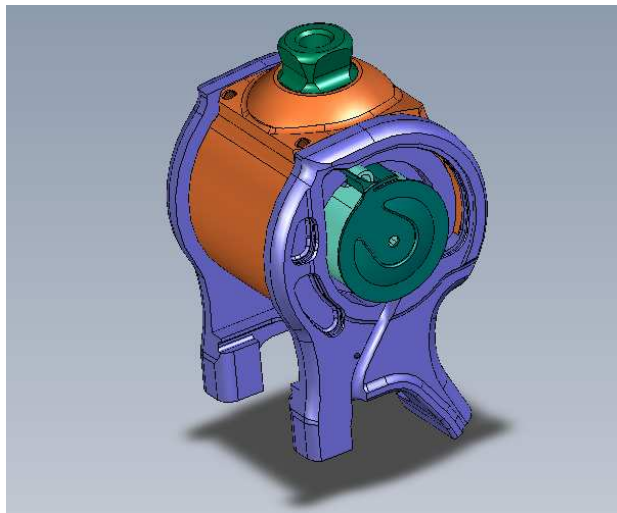


Figure 1. The MR prosthetic knee actuator.

MR fluids have many industrial applications and their variable rheological properties are utilized in various actuators. The prosthetic knee [8,9] is example of such a device, as it uses an MR rotary brake actuator to control the knee's variable stiffness. The actuator's design problem is laid out as multi-objective optimization problem where the aim is to maximize the field-induced strength and to minimize the off-state stiffness and the weight of the actuator. Three objective functions are developed to represent the field-induced braking torque, the off-state minimum stiffness and the weight of the actuator. The optimization problem is a mixed integer-continuous problem with non-linear objective functions and non-linear constraints. The magnetic field inside the brake is described by the Maxwell equations and the problem requires a magnetic FE analysis to evaluate the magnetic flux density in the MR fluid. This makes the optimization problem computationally expensive and limits the total number of evaluations of the objective function describing the

field-induced braking torque. A simple random search algorithm [10] is employed with adjustments to facilitate for a multi-objective optimization problem [10]. The study shows how optimization procedures can aid in the design and further development of the prosthetic knee.

2. STRENGTH OF A PROSTHETIC KNEE ACTUATOR

The applicability of the prosthetic knee joint to heavy amputees is decided by the field-induced strength of the MR actuator. It is therefore important to increase the maximum obtainable braking torque of the actuator to facilitate for a wider usage of the knee.

2-1. Magnetic circuit

An axisymmetric view of the MR actuator is shown in Figure 2. The schematic is based on the original design of Herr and Wilkenfeld [8], and Deffenbaug et al. [9]. The magnetic circuit of the actuator consists of a coil wound around an iron-cobalt alloy core. The magnetic field is directed towards the fluid via iron-cobalt alloy sides that are connected to the each end of the fluid chamber. The fluid chamber is densely packed with steel blades that interact with the MR fluid. The iron-cobalt alloy has a high magnetic saturation value making it well suited material for the magnetic circuit of the MR actuator.

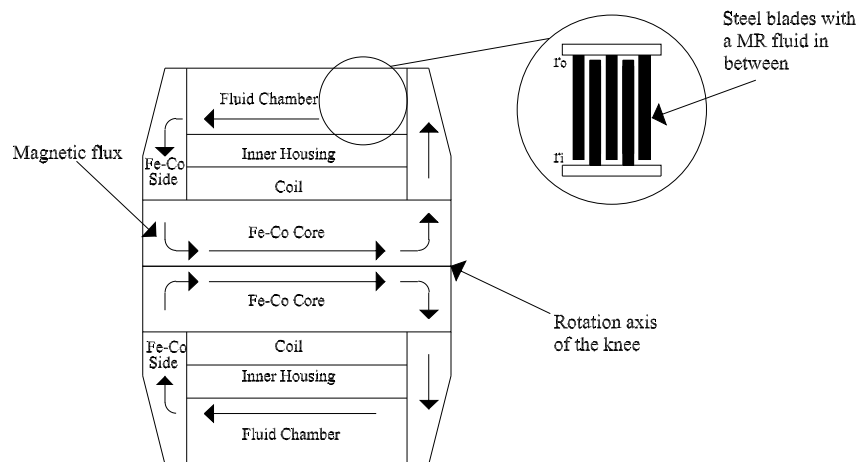


Figure 2. An axisymmetric view of the MR actuator. The schematic is based on the original design of Herr and Wilkenfeld [8], and Deffenbaug et al. [9].

The MR fluid separates the stator from the rotor. The inner parts belong to the rotor while the outer house along with half of the blades belongs to the stator. The stator is connected to the amputee's residual limb while the rotor is connected to the amputee's lower part of the leg (below the knee), producing the relative motion between the stator and the rotor.

2-2. Formulation of the strength

The MR fluid in the actuator, the size of the area that interacts with the fluid, and the magnetic flux density (MFD) in the fluid, are the three factors that affect the strength of the actuator. The

strength analysis is based on shear-yield stress model of a commercially available MR fluid [11]. This reference fluid has a available shear-yield stress curve [7] shown in Equation (1).

$$\tau_y(B) = 26700 - 26400\cos(\pi \cdot B) - 200\sin(\pi \cdot B) \quad (1)$$

The average magnetic flux density (MFD) inside the MR fluid is denoted by B and τ_y is the shear-yield stress in the fluid. A magnetic finite element analysis is used to estimate the MFD. The analysis shows that the variability of the MFD inside the fluid chamber is low. An average MFD value is, therefore, used to determine a single value for the shear-yield stress in the MR fluid.

The field-induced shear yield stress of the MR fluid interacts with steel blades, producing the braking torque. The total area of the blades, interacting with the fluid, is shown in Equation (2) where n_{blades} is the number of blades, r_i and r_o are the inner and outer radii of the fluid chamber, respectively.

$$A_{total} = 2 \cdot n_{blades} \cdot \pi \cdot (r_o^2 - r_i^2) \quad (2)$$

The braking torque is modeled by integrating the shear-yield stress, of the fluid, over half of the total area of blades. Only half of the area is used since only half of the blades are sheared by the MR fluid. The other half is stationary since they are connected to the stator of the actuator. This gives the braking torque of the actuator, shown in Equation (3) [7].

$$T = n_{blades} \cdot \tau_y(B) \cdot 2/3 \cdot \pi \cdot (r_o^3 - r_i^3) \quad (3)$$

The torque due to the post-yield plastic viscosity of the MR fluid is not included in Equation (3) since it is negligible compared to the yield part of the torque.

The magnetic flux density, B , in the fluid is a function of the geometry of the magnetic circuit making the braking torque a function of additional parameters. The design parameters that are considered in this study are shown in Table 1.

Parameter	Description
r_c	Radius of the core
n_{coil}	Number of windings in the coil
t_{s1}	Initial thickness of the sides (at the core)
t_{s2}	Final thickness of the side (at the fluid chamber)
t_s	Start of side thickness reduction (distance from the core)
t_{fc}	Thickness of the fluid chamber
d	Distance between blades in the fluid chamber
n_{blades}	Number of blades in the fluid chamber
t_h	Thickness of inner housing seat (side cut out)

Table 1. The optimization design parameters.

The inner radius of the fluid chamber, r_i , is determined by the radius of the core, the size of the coil and the size of the inner house, shown in equation (4). It is, therefore, not a design parameter.

$$r_i = r_c + \alpha_{coil} \cdot n_{coil} + d_{ih} \quad (4)$$

The thickness of coil per winding is denoted by α_{coil} , the size of the inner housing by d_{ih} . The thickness of the fluid chamber, t_{fc} , is used rather than the outer radius of the fluid chamber, r_o , where $r_o = r_i + t_{fc}$. The current in the coil is not a parameter but is held constant at a maximum value of 1.5 A. Figure 3 shows a schematic view of the actuator with the design parameters considered in the optimization.

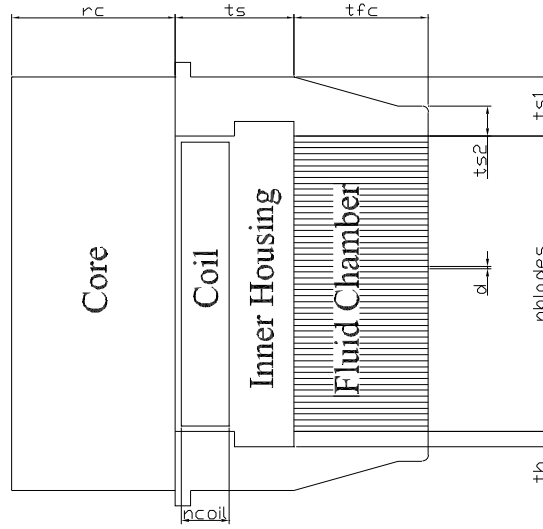


Figure 3. A schematic view of the actuator.

This gives an objective function, f_1 , shown in Equation (5), describing the braking torque of the actuator.

$$\begin{aligned}
 f_1(r_c, t_{fc}, n_{coil}, n_{blades}, t_s, t_{s1}, t_{s2}, d, t_h) \\
 = n_{blades} \cdot \tau_y(B) \cdot 2/3 \cdot \pi \cdot ((r_c + \alpha_{coil} \cdot n_{coil} + d_{ih} + t_{fc})^3 - (r_c + \alpha_{coil} \cdot n_{coil} + d_{ih})^3)
 \end{aligned} \quad (5)$$

Prior to evaluating the objective function, f_1 , a magnetic finite element analysis is used to estimate the MFD, B , in the MR fluid. The constraints of the optimization problem are both linear and non-linear and are the same for all objective functions. The constraints are defined in section 5.

2-3. Magnetic finite element model

A parameterized magnetic finite element model was built to evaluate the MFD in the fluid. The model was built using the ANSYS finite element package. The model is two dimensional and axisymmetric which is a reasonable assumption since the magnetic circuit in the actuator is axisymmetric, apart from a small hole to connect the coil to a voltage generator and three small holes on the sides for fastening pins. The model can be automatically generated, according to the selected design parameters.

The material properties of the model, in the form of B-H curves, are both linear and non-linear making the solution process non-linear. Material properties for the iron-cobalt alloy [12], the steel blades and the MR fluid [11] are shown in Figure 4, Figure 5, and Figure 6, respectively.

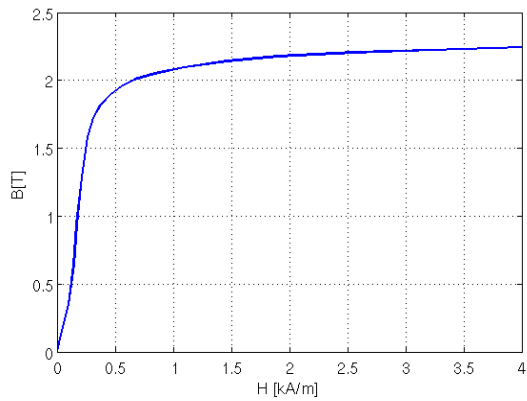


Figure 4. B-H curve for a Co-Fe alloy [12].

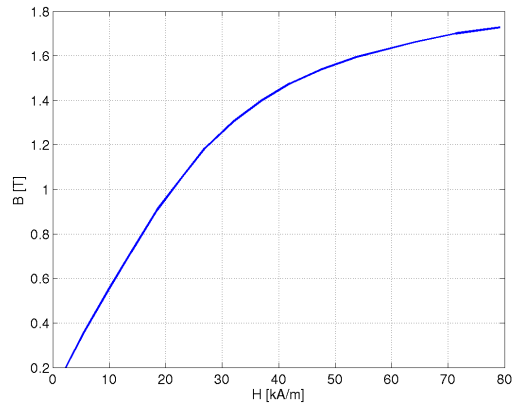


Figure 5. B-H curve for steel.

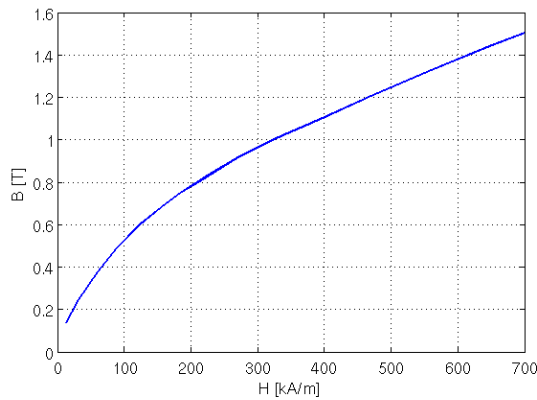


Figure 6. B-H curve for a MR fluid [11].

The inner housing is made of titanium and its magnetic permeability is assumed linear [7], using the same value as for the surroundings of the actuator. The permeability for the titanium and the surroundings is modeled with the magnetic permeability of vacuum, $\mu_0 = 4\pi \times 10^{-7}$ H/m. Figure 7 shows the MFD in the current design of the actuator.

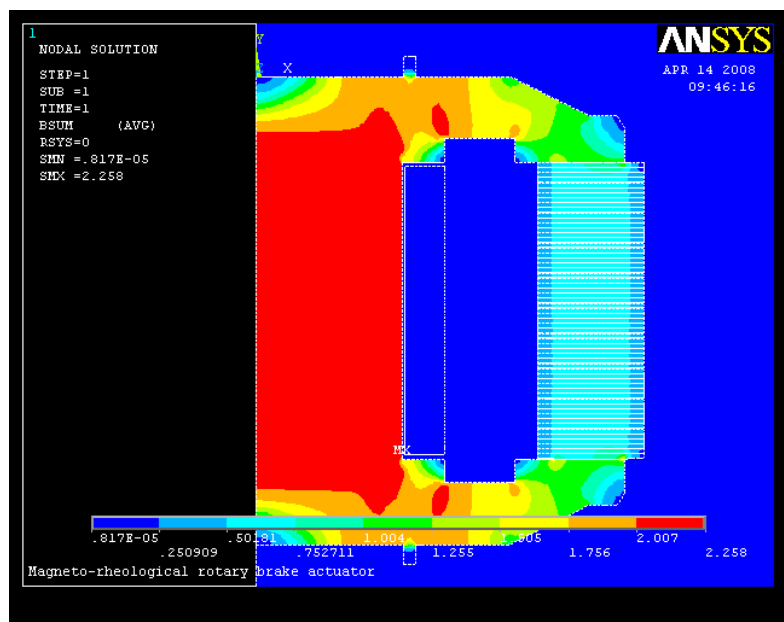


Figure 7. The magnetic flux density in the current design of the actuator.

The core is saturated in the current design of the actuator. The MFD in the fluid is 0.69 Tesla and the aim is to increase this value. Figure 7 shows that the magnetic circuit in the current design of the actuator is not optimal since the circuit should be close to saturation at all points. A detailed

optimization of the magnetic circuit will be performed where the optimization considers the field-induced strength of the actuator, the off-state stiffness of the actuator, along with the weight of the actuator.

3. MINIMUM STIFFNESS OF A PROSHETIC KNEE ACTUATOR

The speed of the prosthetic knee joint, in load-free movements, is decided by the off-state rotational stiffness of the MR actuator. The main factors that affect the off-state rotational stiffness of the knee are: the inner and outer radii of the blades, the number of blades, the gap between the blades, the friction in bearings and oils seals, and the off-state viscosity of the MR fluid. All these parameters are considered apart from the MR fluid which is not a variable. The MR fluid, employed in the knee, is PFPE-based with a 50 % concentration of carbonyl iron particles by mass [5].

3-1. Off-state behavior of the MR fluid

The off-state viscosity of the MR fluid affects the minimum obtainable stiffness of the actuator. Figure 8 shows the off-state viscosity of the employed MR fluid as a function of shear-rate measured with a StressTech rheometer. The figure also shows also the viscosity of the PFPE carrier liquid.

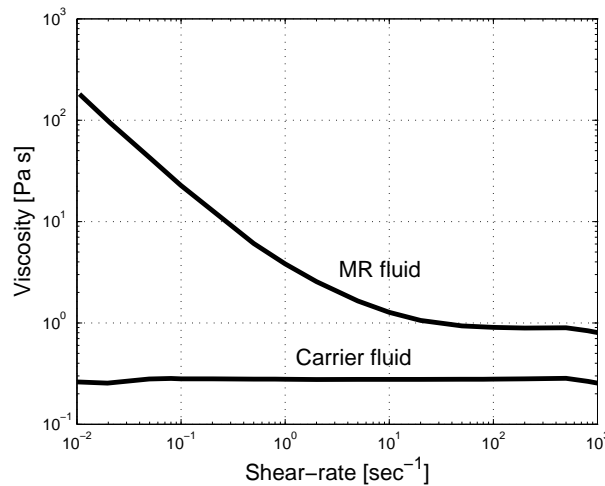


Figure 8. The off-state viscosity of the MR fluid in the actuator.

The working shear-rate of the knee is in the proximity of 1000 s^{-1} . The high shear-rate is due to a small gap between the rotating blades in the actuator. This high working shear-rate is fortunate for the current applications since the actuator is not affected by the high viscosity at low shear-rates. The optimization assumes a constant viscosity, $\mu_{\text{MR}} = 0.9 \text{ Pa s}$, which is a reasonable assumption since Figure 8 shows a constant viscosity at high shear-rates.

3-2. Formulation of the minimum stiffness

Along with the viscosity of the MR fluid, the minimum stiffness of the actuator is decided by the geometry of the fluid chamber, along with friction in oil seals and bearings. The minimum stiffness decides how fast the actuator rotates in load-free movements. Equation (6) describes the minimum obtainable stiffness of the actuator [2].

$$T_{\min} = \frac{\pi \cdot \mu_{MR} \cdot \omega \cdot n_{blades}}{2d} ((r_i + t_{fc})^4 - r_i^4) + T_b + T_o \quad (6)$$

where the off-state viscosity of the MR fluid is denoted by μ_{MR} , and the working shear-rate by ω . The inner radius of the fluid chamber, r_i , is determined by the size of the core, the coil and the inner housing, shown in Equation (4). The torque due to friction in oil seals and bearings is denoted by T_b and T_o , respectively. The torque due to friction is assumed to be constant and, therefore, not considered in the optimization.

This gives an objective function, f_2 , shown in Equation (7), for the minimum obtainable stiffness of the actuator.

$$\begin{aligned} f_2(r_c, n_{coil}, t_{fc}, n_{blades}, d) \\ = \frac{\pi \cdot \mu_{MR} \cdot \omega \cdot n_{blades}}{2d} ((r_c + \alpha_{coil} \cdot n_{coil} + d_{ih} + t_{fc})^4 - (r_c + \alpha_{coil} \cdot n_{coil} + d_{ih})^4) \end{aligned} \quad (7)$$

The parameters of f_2 are the same as in f_1 but fewer since the minimum obtainable stiffness is unaffected by the strength of the magnetic field.

4. WEIGHT OF A PROSHETIC KNEE ACTUATOR

The weight of MR actuator is decisive in the total weight of the prosthetic knee joint and the below-knee prosthetic leg. The selected design parameters all relate to the magnetic circuit and the configuration of the fluid chamber. The total weight of the magnetic circuit, coil and the fluid chamber is shown in Equation (8).

$$M = V_{CoFe} \cdot \rho_{CoFe} + V_{Cu} \cdot \rho_{Cu} + V_{MR} \cdot \rho_{MR} + V_{Fe} \cdot \rho_{Fe} \quad (8)$$

where V is the volume of material and ρ is the density of the material. The materials are: cobalt-iron alloy for the magnetic circuit, copper for the coil, PFPE oil and carbonyl iron for the MR fluid, and steel for the blades in the fluid chamber. Describing the material volumes as function of the design parameters, gives the objective function, f_3 , shown in Equation (9).

$$\begin{aligned} f_3(r_c, t_{fc}, n_{coil}, n_{blades}, t_s, t_{s1}, t_{s2}, d, t_h) = \\ \rho_{CoFe} (\pi r_c^2 (2t_{s1} + L_{coil}) + \pi((r_c + t_s)^2 - r_c^2) \cdot 2t_{s1} + \pi((r_i + t_{fc})^2 - (r_c + t_s)^2)(t_{s1} - t_{s2})) + \\ \rho_{Cu} (n_{coil} \cdot 2\pi r_c \cdot \pi(d_{coil}/2)^2) + \rho_{MR} (n_{blades} \cdot d \cdot \pi((r_i + t_{fc})^2 - r_i^2)) + \\ \rho_{Fe} ((L_{coil} - n_{blades} \cdot d) \cdot \pi((r_i + t_{fc})^2 - r_i^2)) \end{aligned} \quad (9)$$

where L_{coil} and d_{coil} are constants representing the length and the diameter of the coil wire, respectively. The inner radius of the fluid chamber, r_i , is determined by size of the core, coil and the inner housing as shown in Equation (4). The length of the coil equals the length of the fluid chamber as is shown in figure 3. The optimization aims to minimize the weight, promoting lightweight designs for patients comfort and reducing the cost of prosthetic knee.

5. MULTI-OBJECTIVE DESIGN OPTIMIZATION

A simple random search algorithm [10] is employed to map the trade-offs between the three design objectives. The results of the optimization procedure are a basis for informed design decisions about the MR actuator. These decisions are decisive on qualities of the prosthetic knee but do not lead to a single optimal solution. Since there is no single optimal solution of a multi-objective optimization problem the solution space is explored by inspecting the pareto trade-off surface [10]. The objective space is three dimensional since the objective functions are three and the trade-off surface is a surface in this three dimensional space. The trade-off surface contains all solutions that are found to be non-dominated. A non-dominated solution is a solution that is optimal in the sense that no other found solution is strictly better. Strictly better means that all three objective functions need to be better. This gives rise to a set of solutions that are pareto-optimal and give valuable information about the trade-offs between the three design objectives.

5-1. Problem definition

The optimization problem is stated as:

max $f_1(\mathbf{x})$ and min $f_2(\mathbf{x})$ and min $f_3(\mathbf{x})$.

subject to:

$$2\pi \cdot r_c \cdot n_{coil} < \pi \cdot 19.05 \cdot 352; \text{ Maximum length of a coil wire based on existing design.}$$

with lower and upper bounds:

$$9 \text{ mm} \leq r_c \leq 13 \text{ mm}$$

$$250 \leq n_{coil} \leq 400$$

$$5 \text{ mm} \leq t_{s1} \leq 7 \text{ mm}$$

$$2 \text{ mm} \leq t_{s2} \leq 4 \text{ mm}$$

$$12 \text{ mm} \leq t_s \leq 18 \text{ mm}$$

$$4 \text{ mm} \leq t_{fc} \leq 7 \text{ mm}$$

$$15 \text{ }\mu\text{m} \leq d \leq 25 \text{ }\mu\text{m}$$

$$59 \leq n_{blades} \leq 79$$

$$0.4 \text{ mm} \leq t_h \leq 0.8 \text{ mm}$$

5-2. Optimization

The search algorithm was allowed 600 iterations where 222 solutions were found to be feasible and 578 were found to be infeasible and therefore rejected without evaluating the objective functions. An evaluation of maximum obtainable braking torque, f_1 , is computationally expensive due to the magnetic finite element analysis. Each evaluation of f_1 takes approximately three minutes making the total optimization time, approximately 11 hours. Of the 222 feasible solutions, 38 were found to be non-dominated, that is, no other solution was better with respect to all three objective functions.

5-3. Results

Table 2 shows the three solutions that resulted in a maximum braking torque, minimum off-state stiffness and minimum weight.

Values			Parameters									
f_1	f_2	f_3	r_c	n_{coil}	t_{s1}	t_{s2}	t_s	t_{fc}	d	n_{blades}	t_h	
76.3	13.7	0.55	12.4	270	6.1	2.9	16.4	7.0	22	75	0.75	
32.2	3.6	0.37	9.3	350	6.0	2.4	16.4	4.2	25	63	0.45	
32.1	5.9	0.26	9.2	300	5.0	3.2	12.2	4.2	16	71	0.7	

Table 2. Three solutions containing a maximum braking torque, a minimum off-state stiffness and a minimum weight.

The first solution in Table 2 has a braking torque of 76.3 Nm which was the highest achieved. The second solution has off-state stiffness of 3.6 Nm which was the lowest achieved and the third has a weight of 0.26 kg which was the lowest achieved. All these three solutions are extremes and unpractical since the extreme values are obtained on the expense of other design objectives. The solution with the highest braking torque has a very large core and large fluid chamber giving it a clear advantage in strength but scoring poorly in off-state stiffness and weight. The solution with the lowest off-state stiffness has a small fluid chamber and large gap between the blades giving it a clear advantage in off-state stiffness but scoring poorly in strength. The solution with the lowest weight has a small magnetic circuit and a small fluid chamber giving it a clear advantage in weight but scoring poorly in strength.

Interestingly for the designer, the optimization process has produced a whole set of solutions that all are optimal with respect to the three design objectives. Figure 9 shows a surface in three dimensions where the x-axis is the off-state stiffness, y-axis is the weight and the z-axis is the braking torque. The figure is obtained using a cubic interpolation on the 38 solutions found to be non-dominated and pareto-optimal.

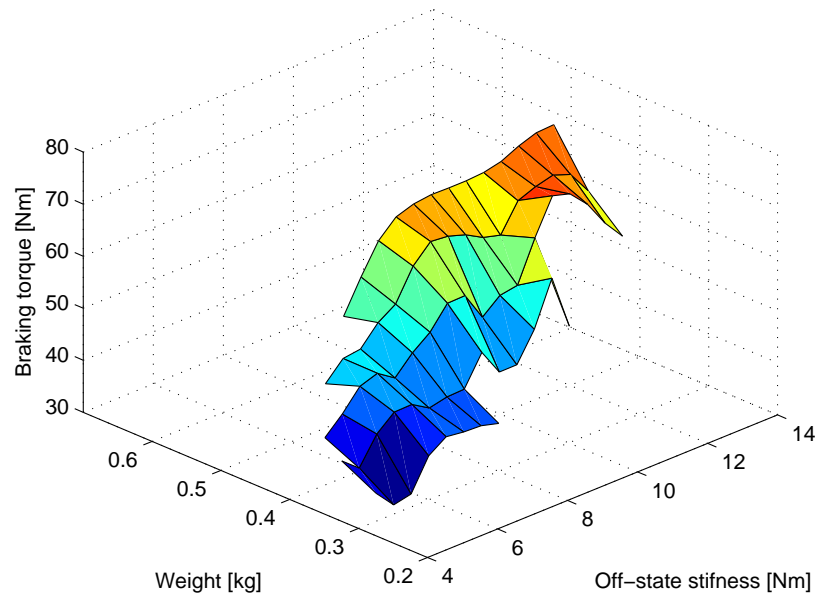


Figure 9. A surface describing non-dominated solutions.

Figure 9 can give rise to various interpretations. For example, the designer can decide to allow an off-state stiffness of 10 Nm. This design decision gives a fixed point on the x-axis allowing the designer to read from the graph what maximum braking torque to expect as a function of the weight of the actuator. Another approach would be to decide what the maximum weight of the actuator should be allowing the designer to see what maximum braking torque to expect as a function of the off-state stiffness. Figure 9 is, therefore, a good basis for informed design decision when designing the MR actuator.

To compare this to existing design of the actuator where the braking torque requirements are approximately 40 Nm [7]. With a 40 Nm braking torque requirement, the pareto-surface gives a minimum of 6.3 Nm for the off-state stiffness. This is the lowest off-state stiffness to expect, or the minimum obtainable off-state stiffness, given the stated braking torque requirement of the knee.

6. CONCLUSIONS

The study shows how multi-objective design techniques can aid the designer in making informed design decision about the MR prosthetic knee actuator. The design is a trade-off between many objectives which aims to select the right balance for the main objectives. The design of the prosthetic knee can be approach in various ways. The approach taken in this study is to map the trade-offs between three design goals: the field-induced strength, the off-state stiffness, and the weight of the actuator. A surface in three dimensional space is presented that shows how the optimal values of the three design goals relate. This can be used in making informed design decisions about the MR prosthetic knee actuator.

It is important to tune the magnetic circuit of the actuator to the field-induced properties of the employed MR fluid. The maximum shear-yield stress of the fluid decides the optimal layout of the magnetic circuit. Improvements of the magnetic circuit beyond the maximum obtainable shear-yield stress of the MR fluid are unnecessary and are on the expense of the weight of the actuator. However, it is advisable, due equipment wearing, that the magnitude of maximum magnetic flux density in the fluid chamber exceeds the saturation value of the MR fluid by a small margin.

Valuable simulation data has been obtained that can aid designers in further improvements of the prosthetic knee actuator.

ACKNOWLEDGEMENTS

This work is funded by the University of Iceland research fund and supported by Ossur Inc.

REFERENCES

1. Jolly, M. R., J. W. Bender and J. D. Carlson, "Properties and Applications of Commercial Magnetorheological Fluids," *Journal of Intelligent Material Systems and Structures*, Vol. 10, pp. 5-13 (January 1999).
2. Gudmundsson, K. H., F. Jonsdottir and S. Olafsson, "The Viscosity of Magneto-Rheological Fluids in a Prosthetic Knee Actuator," *Proceedings of 11th International Conference on New Actuators*, (June 2008).
3. Barber, D. E., J. D. Carlson and R. Wilder, "Prototype MR Mounts Utilizing Glycol-Based MR Fluids," *Proceedings of 11th International Conference on New Actuators*, (June 2008).
4. Goncalves, F. D., "Characterizing the Behavior of Magnetorheological Fluids at High Velocities and High Shear Rates," Ph. D. Dissertation, Virginia Polytechnic Institute and State University, (January 2005).
5. Hsu, H. H., C.R. Bisbee III, R.J. Lukasiewics, M.W. Lindsay and S.W. Prince. "Magnetorheological Fluid Compositions And Prosthetic Knees Utilizing Same," *US Patent 7,101,487*, (September 2006).
6. Thorarinsson, E. T., F. Jonsdottir and H. Palsson, "Finite element analysis of a

- magnetorheological prosthetic knee”, *Proceedings of the ASME Summer Bioengineering Conference*, Florida, (June 2006).
7. Gudmundsson, K. H., F. Jonsdottir, H. Palsson and S. G. Karlsson, “Optimization of a Magneto-Rheological Rotary Brake, ”*Proceedings of 3rd ECCOMAS Thematic Conference on Smart Structures and Materials*, (June 2007).
 8. Herr, H. and A. Wilkenfeld, “User-adaptive control of a magnetorheological prosthetic knee,” *Industrial Robot: An International Journal*, Vol. 30, pp. 42-55 (January 2003).
 9. Deffenbaug, B. W., H. Herr, G. A. Pratt and M. B. Wittig, “Electronically controlled prosthetic knee,” *U.S. Patent 6,764,520*, (July, 2004).
 10. Coello, C. A. C., G. B. Lamont and D. A. Van Veldhuizen, “Evolutionary Algorithms for Solving Multi-Objective Problems,” *Springer*, 2nd Edition, (2007).
 11. Lord Corporation, Gary, N.C., U.S.A.
 12. Information on http://www.vacuumschmelze.de/dynamic/docroot/medialib/documents/broschueren/htbrosch/Pht-004_e.pdf.